2018-01-1514 Published 13 Jun 2018

# Application and Simulation of Micro-Perforated Panels in HVAC Systems

**Sebastian Floss and Manfred Kaltenbacher** Vienna University of Technology

**Gerhard Karlowatz** Liebherr-Transportation Systems GmbH

***Citation:*** Floss, S., Kaltenbacher, M., and Karlowatz, G., "Application and Simulation of Micro-Perforated Panels in HVAC Systems," SAE Technical Paper 2018-01-1514, 2018, doi:10.4271/2018-01-1514.

## Abstract

To reduce noise in a HVAC system for railway application the usage of micro-perforated panels (MPP) is proposed. MPPs offer some favorable characteristics, like robustness and durability in harsh environments and the possibility to optimize absorption in desired frequency bands. The underlying acoustic mechanism can be modelled via an equivalent fluid in accordance with the Johnson-Champoux-Allard (JCA) approach, treating the MPPs as a porous material with rigid frame. This allows to conduct the necessary acoustic pre-evaluation in complex HVAC application scenarios in order for the MPPs to substitute the commonly used foam and fibrous absorber materials.

## Introduction

The reduction of noise emissions in HVAC systems is still a demanding challenge. One has to deal with harsh environments, the absorber must nevertheless last for many maintenance cycles and satisfy demanding fire protection standards such as the EN 45545-2. Broadband sound reduction is desired and the pressure drops induced by the absorber materials should be small. Usually foam and fibrous materials are used to meet most of these tasks.

We propose the application of micro-perforated panels to substitute the standard absorber materials, since they exhibit characteristics being well appropriate to be used in HVAC systems:(1) They can be made out of various robust materials; (2) they are passively tunable to a special frequency band and broadband absorption is a matter of arrangement, which, however, must be examined beforehand, since a single MPP is only narrow band absorbing; (3) by applying the Finite Element method (FEM) in combination with an equivalent fluid approach, the sound absorbing properties of MPP configurations in complex environments can be pre-evaluated.

The idea to use MPPs as acoustic absorbers goes back to Maa et al. and the acoustic behavior of perforations in plates has already been extensively studied by Ingard et al. (see [1, 2]). We demonstrate the applicability of these plates on the example of a silencer section in a HVAC system for railway application. Our results show that MPPs can substitute the conventional absorbers up to a certain frequency band. For pre-evaluating MPP arrangements with different number of layers and layer distances, with the goal of broad band absorption, targeting a certain frequency band and minimal overall layer thickness, it is sufficient to use the transfer matrix method (TMM) for conducting parameter studies. The method assumes plane wave propagation and an incident angle perpendicular to the absorber material. Depending on the dimensions of the HVAC duct cross section, one can identify a cut-on frequency from which higher order modes can propagate. These higher order modes can be represented by inhomogenous waves, with nonparallel equiphase and equiamplitude planes propagating at different directions (plane wave decomposition) [3]. Unless one partitions the MPP backing volume with a fine honeycomb-like structure, one must assume extended reaction for the combination of MPP and backing air volume in contrast to the local reaction assumption for many porous materials where the surface impedance is not dependent on the incident angle [4].

MPPs may also be used as flow guiding structures. In this scenario, several layers of MPPs and air volume in form of, e.g., a flow guiding vane would be placed in section of a duct where the flow changes direction, this is commonly known as baffle silencer. In another application case one single MPP could be placed where the duct cross section suddenly changes. The change of cross section induces an impedance jump which causes a reflection of sound wave. This expansion chamber principle is used in automotive mufflers and produces sound reduction where the attenuated frequency band depends on the length of the expansion and the reduction peak depends on the ratio of the cross sections. In the HVAC application case the MPPs would guide the flow, hence reduce the occurring pressure drop. At the same time the panel would increase and by partioning the backing chambers or mutlilayer arrangement broaden the sound reduction at this section.

# Acoustic Mechanism of MPPs

The ideal dissipative absorber material has an acoustic resistance close to the characteristic impedance of air, so that most of the wave energy can penetrate the material where the wave energy is dissipated by friction. The plates under consideration consist of micro-perforations in the submillimeter range and these show such an ideal behavior as long as the acoustic viscous boundary layer ($\delta = \sqrt{2\eta_0 / \omega}$) is larger than the perforation radii, where the friction losses are induced (see [5]). Thereby, $\eta_0$ denotes the dynamic viscosity of air and $\omega$ the angular frequency. However, the acoustic reactance of the moving air volume in the perforations is small. By combining the plate with an air volume of length $D$ having impedance

$$Z_{\text{air}} = -j \cot \omega D / c_0$$

with speed of sound $c_0$, the reactance can be increased (see Figure 1). The absorption peak depends on perforation radius size, whereas the location of the peak in the absorption spectrum can be tuned with the length $D$. Broad band sound absorption can be achieved by either combining multiple layers (see Figure 3) in a series arrangement or partioning the air volume, hence making the combination of MPP and air volume more locally reacting (see [6]). Partioning the backing volume with honey-combs would be the optimal scenario. The MPP itself can be made out of various materials and it is a matter of production costs how to manufacture the perforations and a generic perforation radius design would be an additional optimization step. These first studies, however, were done on commercially available MPPs (see Figure 2) with slitted perforations and a thickness of about 1.6 mm. The involved physical phenomena can be described and modelled

**FIGURE 1** MPP in front of air volume with length $D$

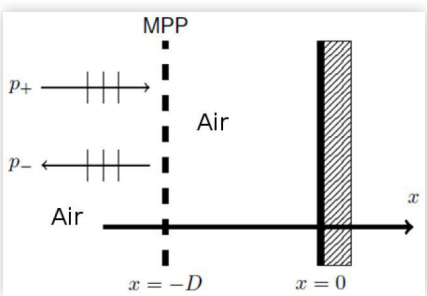


© SAE International

**FIGURE 2** Commercial MPP absorber (Acustimet™), slit shaped holes with slit length of about 5 mm, [6]

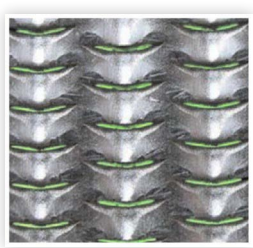

© SAE International

**FIGURE 3** Measurement (red) and Simulation (blue) of slitted MPP with 60 mm air cavity; Simulation (black) of double layered MPPs

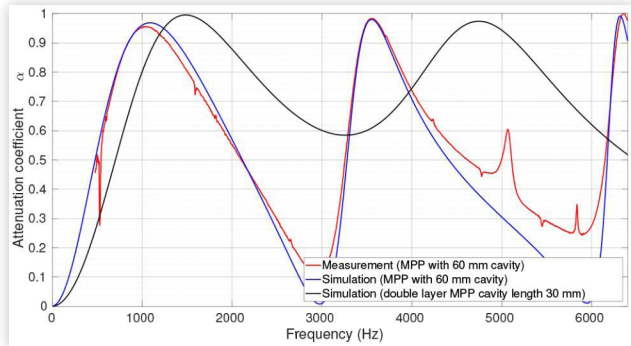


© SAE International

by assuming cylindrical, straight pores. Therefore, one has to determine effective parameters for the slitted perforation case, e.g., by fitting simulation and measurement of the attenuation coefficient $\alpha$ (see Figure 3) using an impedance tube with transfer function method according to [7]. The approach is described by Jaouen et al. in [8].

# Perforation physics

The physical phenomena involved are described in Figures 4 and 5. The classical approach is to evaluate the surface impedance ($Z_n = R_n + j\omega M_n$) of a single perforation and assuming normal incident impinging waves (see [5]). The resistive part ($R_n$) is induced by the viscous effects occurring within the perforation due to the viscous boundary layer and around its edges at the panel surface due to the distortions of the acoustic flow. The reactive part $M_n$ accounts for the motion of an air cylinder, which is thicker than the thickness of the plate (perforation depth $t$, see Figure 4). This means additional mass loading and in combination with flow distortion make the air in the neck heavier and more difficult to move. The inertial effect is captured by adding correction length $\epsilon$ to the neck depth at both sides. Interaction between perforations (overperforation, see Figure 5) also occurs when the porosity $\phi$ increases and the moving fluid particles of an opening are perturbated by neighboring openings (see [9] and [10]). Therefore, $Z_n$ is corrected with a Fok-like function $\Psi_{\text{Fok}}(\xi)$, where $\xi$ depends on the porosity $\phi$. The influence of a mean flow field on the acoustics of the MPP liner is not considered here, since the occurring flow velocities in the railway application case were negligible (< 20 m/s).

**FIGURE 4** Correction length for single perforation

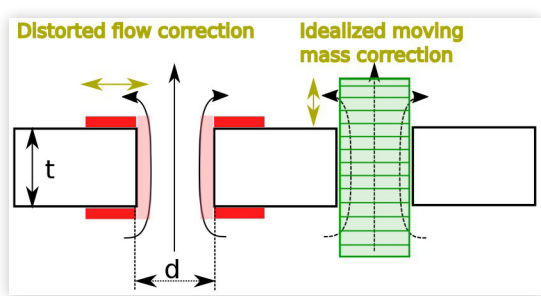


© SAE International

**FIGURE 5** Correction for overperforation, [6]

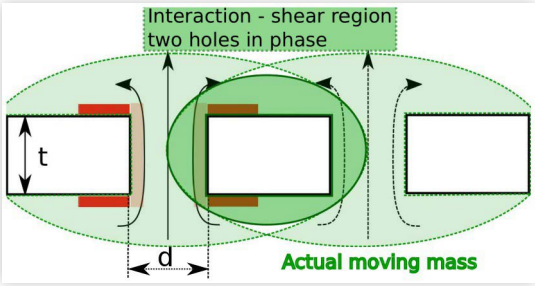




## Modeling

The characteristic impedance $z_{MPP} = Z_{MPP}/\phi$ of an MPP-layer, with $Z_{MPP}$ as the impedance of single perforation, under normal incidence impinging waves without the influence of mean flow, but incorporated correction lengths (see [6, 3, 9]) may be computed by

$$z_{MPP} = \frac{j\omega\rho_0}{\phi}\left[t + \frac{2\epsilon}{\Psi_{Fok}(\xi)}\right]\left[1 - \frac{2}{x\sqrt{-j}}\frac{J_1\left(x\sqrt{-j}\right)}{J_0\left(x\sqrt{-j}\right)}\right]^{-1}. \quad (1)$$

In (1) $\rho_0$ denotes the mean density of air, $J_1$ and $J_0$ are Bessel functions of the first and zeroth order and $x = \frac{d}{2}\sqrt{\frac{\omega\rho_0}{\mu_0}}$ is the ratio of the radius and the viscous boundary layer thickness. It compares inertia forces to viscous forces and is also termed the acoustic Reynolds number (see [1, 11]). The derivation of the third term in (1) is desribed in [3].

The characteristic impedance $z_{MPP}$ can be derived in a more general way (Johnson-Champoux-Allard model) if the viscous and thermal effects of the perforations are incorporated in an effective frequency dependent density $\rho_{eff}$ and bulk modulus $K_{eff}$ of an equivalent fluid. The MPP is treated as porous material with rigid frame (see [12]). The material's microstructure is homogenized over the volume. This approach is valid as long as the occurring shortest wave length is much larger than the characteristic length scales of the microstructure. The model requires flow resistivity $\sigma$, viscous and thermal characteristic length $\Lambda, \Lambda'$ and tortuosity $\alpha_\infty$ as parameters. According to [3, 8] for cylindrical shaped pores these parameters can be calculated from the radius $r = d/2$ of the pores and the overall porosity $\phi$ with.

- $\Lambda' = \Lambda = r; \sigma = \frac{8\eta_0}{\phi r^2}$
- $\alpha_\infty = 1 + 2\frac{\epsilon}{t}$
- $\epsilon = \left(1 - 1.13\xi - 0.09\xi^2 + 0.27\xi^3\right)\frac{8r}{3\pi}$ mit $\xi = \sqrt{\frac{\phi}{\pi}}$

resulting in

$$\rho_{eff}(\omega) = \frac{\alpha_\infty\rho_0}{\phi}\left[1 - j\frac{\sigma\phi}{\omega\rho_0\alpha_\infty}\sqrt{1 + \frac{4\alpha_\infty^2\eta_0\rho_0\omega}{\sigma^2\Lambda^2\phi^2}}\right] \quad (2)$$

$$K_{eff}(\omega) = \frac{\gamma p_0/\phi}{\gamma - (\gamma - 1)\left[1 - j\frac{8\kappa}{\Lambda'^2 c_p\rho_0\omega}\sqrt{1 + j\frac{\Lambda'^2 c_p\rho_0\omega}{16\kappa}}\right]^{-1}}. \quad (3)$$

In (3) $\kappa$ denotes the thermal conductivity and $\gamma$ the heat capacity ratio of air. One can compute the frequency dependent characteristic impedance $z_{MPP} = \sqrt{\rho_{eff}K_{eff}}$ and frequency dependent wave number $k_{MPP} = \omega\sqrt{\rho_{eff}/K_{eff}}$ of the MPP-layer.

These values were then used to simulate layers of MPPs and air volumes in the plane wave case with the transfer matrix method (TMM).

# Noise Reduction in a HVAC System for Railway Application

Figure 6 shows the sketch of the latest generation of a HVAC system for railway application. The system can roughly be grouped into three sections. The noise is generated by a compressor and a turbine, originally developed for aircrafts, to cope with the large necessary mass flows, since the system works with air as convector medium and water vaporizing, producing the cooling effect. The **Turbine Out** section has been designed for sound absorption purposes to reduce sound power at least by 10 dB until the sound reaches the **Mixing chamber** section to finally be emitted to the passenger cabin via the **Return Air** outlet(see Figure 6).

## Application of MPPs

Multilayered MPP designs were pre-evaluted with the TMM taking into account broadband absorption and a minimal absorber volume. The minimal absorber volume is determined by the thickness (30 mm) of a generally used fibrous absorber material. This is due to the important criterium of a low pressure drop between the silencer inlet and outlet. The MPP arrangements were installed in the silencer section (see Figure 7). The positions are marked with 1 to 4.

At position 1 and 3 a double layer arrangement was placed and at position 2 two triple layers arrangements (see Figure 8). At position 4 a single MPP layer replaces the mounting of fibrous material.

**FIGURE 6** Sketch of HVAC system, railway application

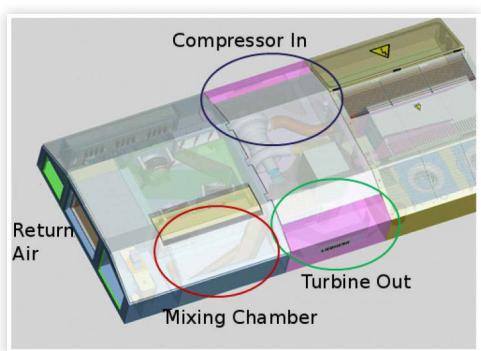

**FIGURE 7** MPP positions in the **Turbine Out** silencer section

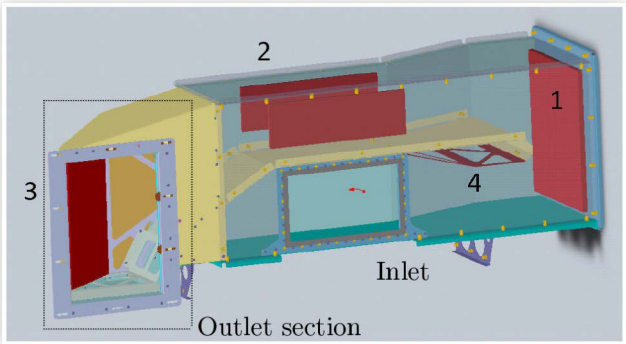




**FIGURE 8** Used triple (left) and double (right) layered MPP configurations

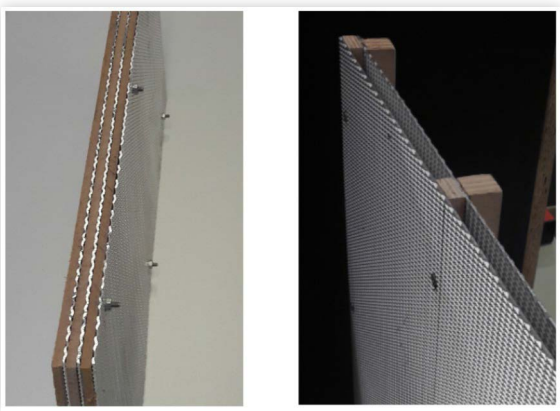



## Test Setup

The silencer section was placed in an approximated free field environment (see Figure 9) with a mean reveberation time of 0.15 sec. in a frequency range beyond 500 Hz (see [17]). Two microphones were used to measure the sound pressure level (SPL) at 60 and 120 cm above the outlet of the silencer. The measurements were repeated three times for every microphone position and averaged in the frequency domain. The microphone positions above the outlet and the loud speaker mounted on the inlet can be seen in Figure 10.

**FIGURE 9** Acoustic chamber with approximated free field environment, [17]



**FIGURE 10** Measurement setup with two microphones

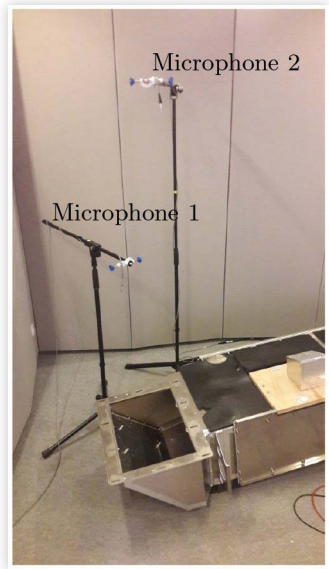




## Results

Figure 11 shows the 1/3 octave band averaged SPL spectrum of different MPP arrangements in comparison to a foam absorber material (blue curve). The foam absorber was installed on the circumference within the outlet section (Figure 7) of the silencer. The black curve shows the case of no damping material applied. The red curve shows the effect of double layered MPPs installed at positions 1 and 3. If one adds a triple layer MPP at position 2 (green curve), one gains a significant increase in sound reduction at mid-frequencies 2500, 3150 and 4000 Hz.

In Figure 12 the red curve shows the case of multilayered MPPs from Figure 11 with an additional single layer MPP at position 4. The green curve indicates the usage of the standard fibrous material at the same positions, except position 4. Taking into account that the standard material will additionally be covered by a protective sheet, which will reduce the absorption capabilities, the MPPs can substitute fibrous or foam material up to a mid-frequency of 6300 Hz.

**FIGURE 11** 1/3 Octave band at microphone 2, 120 cm above the outlet; comparison of double and triple MPP layer to foam absorber

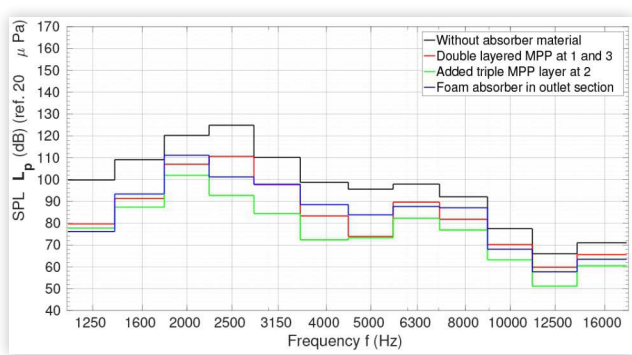

**FIGURE 12** 1/3 Octave band at microphone 2, 120 cm above the outlet; double, triple MPP layer and one layer at Pos. 4 in comparison to fibrous absorber material

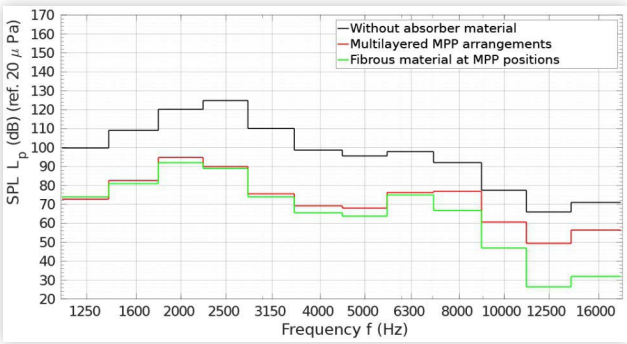


## Simulation of a Complex Sound Field

As previously seen the sound absorption properties of MPP-layers in a simple planar liner configuration can be estimated with the plane waves assuming TMM (plane waves have equiphase and equiamplitude planes perpendicular to the direction of propagation, also called homogenous plane waves, see [3, 4]). But the prediction of sound power reduction for the entire silencer for a certain set of MPP configurations in a 3D environment cannot be accomplished using plane wave assumption for frequencies higher than the cut-on frequency. Also the wide usage of honey-combs to enforce a local reaction of MPP and backing air chamber might not be practically realizable.

As additionally mentioned in the introduction the application of MPPs is not limited to substitute liner arrangements that cover a large planar area. They can be used as flow guiding baffle silencers. Additionally the backing chamber geometry might not have rectangular shape or there could be no backing chamber at all if a single MPP would simply substitute a flow guiding unperforated metal plate. The introductorily mentioned expansion chamber principle with an MPP as guiding plate is another example of an unconventional absorber design which can only be modelled analytically or with the TMM below the cut-on frequency.

In the case of the HVAC system as shown in Figure 7 (the inlet has a rectangular cross section with a height H = 30 cm and a width of B = 22 cm) above a frequency of about 600 Hz higher order modes will propagate.

These higher order modes correspond to equiphase and equiamplitude plane waves impinging on the the absorber at oblique angles or inhomogenous waves with nonparallel equiphase and equiamplitude planes (see Figure 13). The wave number vector **k** has three components indicating that the plane waves can propagate at any direction. The complex sound pressure $\hat{p}_a$ can be described by

$$\hat{p}_a(x_1,x_2,x_3,t) = \hat{A}exp\left[j\left(-k_1x_1 - k_2x_2 - k_3x_3 + \omega t\right)\right]$$

**FIGURE 13** Symbolic representation of an inhomogenous plane wave with **k** parallel to plane $x_3 = 0$, [3]

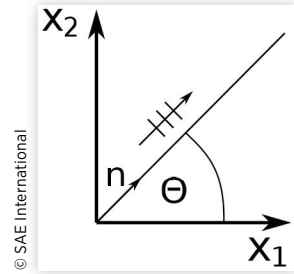


**FIGURE 14** Layer of fluid with thickness D backed by rigid wall, [3]

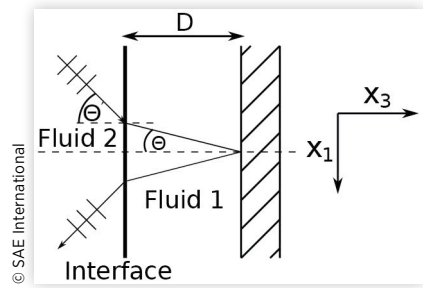


with $k_{i=1,2,3}$ as wave number components, $\omega$ is the angular frequency, $t$ represents the dependence on time and $\hat{A}$ is the the complex amplitude. In Figure 13 **n** denotes the unit vector of direction of propagation.

The incident angle dependence of the effective surface impedance of a layer of fluids with different absorption properties is shown in Figure 14. An equiphase and equiamplitude plane wave impinges from Fluid 2 (e.g. non disspative with real wave number $k$) under angle $\Theta'$, is refracted by Fluid 1 (disspative medium with complex wave number $k$) under angle $\Theta$, reflected by the rigid backing and again refracted into Fluid 2. With $k^2 = k_1^2 + k_2^2 + k_3^2$ and assuming $k_2 = 0$ for propagation in the $x_2 = 0$ plane the following relations can be computed:

$$k_1 = k_1' = k'\sin\Theta' = k\sin\Theta \quad k_3 = \left(k^2 - k_1'^2\right)^{1/2}$$

This results in

$$z_{\text{Interface}} = -z_{\text{Fluid 1}}\frac{k}{k_3}j\cot k_3 D$$

The effective surface impedance of a MPP in series with a backing air volume would therefore also become incident angle dependent, but these angles are unkown in a pre-design stage.

To be able to pre-evaluate the effect of MPP design in the oblique incidence case for arbitrary complex geomtrical setups, the sound pressure field $\hat{p}_a(\boldsymbol{x},t)$ can be simulated with the Finite Element (FE) method solving a modified Helmholtz equation with complex density $\rho_{\text{eff}}$ and complex bulk modulus $K_{\text{eff}}$ (see [13, 14]):

$$\frac{\omega^2}{K_{\text{eff}}}\hat{p}_a + \nabla\cdot\frac{1}{\rho_{\text{eff}}}\nabla\hat{p}_a = 0 \tag{4}$$

This formulation of the Helmholtz equation can handle computational domains with varying density. The derivation of (4) can be found in [16].

## Test Setup

To test if the sound absorption properties can correctly be simulated in the oblique incident case and more complex absorber arrangements, a measurement setup with a modified expansion chamber and an variable attachment has been designed. The attachment allows to test different MPP arrangements (partitioned, multilayered) and measure the transmission loss (TL) of the expansion chamber (see Figure 16). The measurement principle uses TMM as described in [15] (see Figure 15).

The measureable frequency range has been augmented to 8 kHz by using smaller dimensions (quadratic cross section with a = 2 cm) of the measuring channels where the microphone pairs are flush mounted (see Figure 16). By this the propagation of plane waves up to a cut-on frequency of about 8 kHz is guaranteed. The distance of the microphones had to be adjusted as well (see [7]) to be able to distinguish the pressure amplitude differences at the microphone pairs. The quadratic cross section of the expansion chamber has a side length b of 9 cm which gives a cut-on frequency of about 3.8 kHz ($f_c = c_0/(2b)$). The TMM requires measuring the same configuration twice, each time with a different end section, indicated by A and B in Figure 15.

**FIGURE 15** TMM schematic with microphone positions 1 to 4

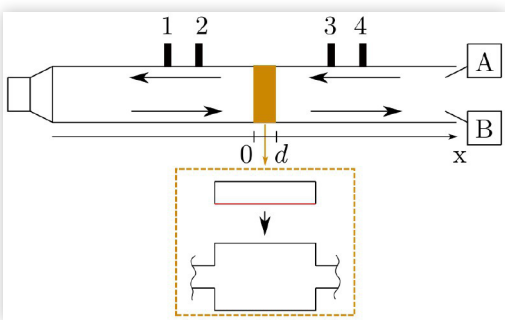




**FIGURE 16** Expansion chamber with attachment

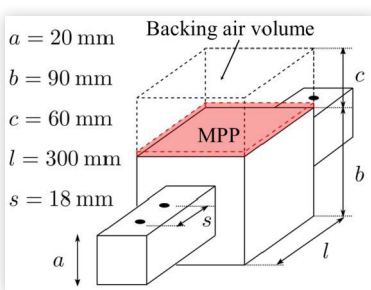




## Results

The case of a single MPP layer, single MPP layer with partitioned air cavity and a four layer arrangement parallel to the chamber axis are shown in Figures 17, 18 and 19.

The values for effective density and bulk modulus were calculated by fitting the measured attenuation coefficient

**FIGURE 17** Measured (red) and simulated (blue) TL of one MPP in the attachment

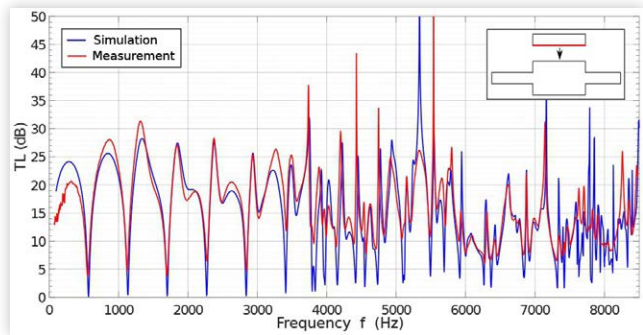




**FIGURE 18** Measured (red) and simulated (blue) TL of four MPP layers in the expansion chamber

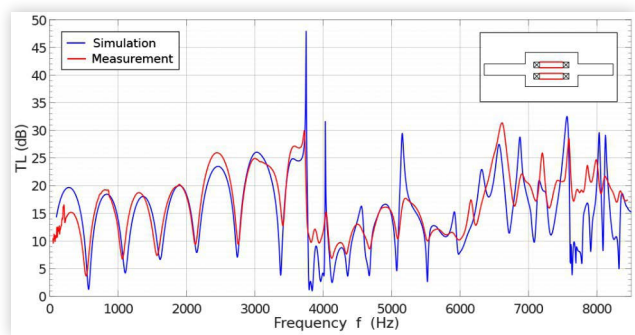




**FIGURE 19** Measured (red) and simulated (blue) TL of one MPP layer with partitioned backing chamber in the attachment

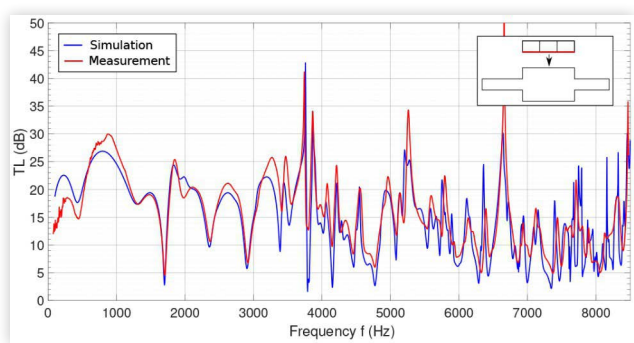

curve of an MPP sample with backing air cavity depth of 6 cm in an impedance tube with the TMM simulation of the same layer arrangement (normal incidence plane wave case) (see Figure 3). The curves were fitted up to a frequency of 6.4 kHz which is the maximum frequency range that can be achieved by an impedance tube with 2.9 cm diameter (see Figure 3). The values for $\rho_{eff}$ and $K_{eff}$ up to 8 kHz were extrapolated with the fitted model. One can see that there is generally good agreement between measurement and simulation up to a frequency of 6.4 kHz. However, there is a larger discrepancy between measurement and simulation in the case of a single MPP (Figure 17). The first two lobes in the spectrum are underestimated by 5 dB. This may be caused by inadequate simulated thickness of the MPP. One can also observe, that arranging a single MPP in such a way way that plane waves graze past the absorber is not optimal for the overall sound reduction. The expansion chamber without absorber material produces TL-lobes with 20 dB peaks up to the cut-on frequency. This can be calculated analytically with the ratio of the cross sections (a and b) (see Figure 16). Figure 18 shows that the absorption in the higher frequency range (oblique impinging waves) can be augmented by using a baffle silencer like structure, whereas the absorption band can be broadened by partitioning the backing cavity (see Figure 19). In the case of 4 MPPs (layered baffle silencer structure) arranged in the expansion chamber, however, one can see a stronger discrepancy between measurement and simulation, starting at around 6 kHz. This indicates that the model might have to be improved further for the case of MPPs being used without an enclosing air cavity.

## Conclusions

The application of MPPs in an HVAC scenario has been investigated. Comparing the results of a multilayer MPP configuration with the standard fibrous and foam absorber material, we show that MPPs can substitute the standard material up to a certain frequency band. Nevertheless, one has to take into account that the fibrous material will be covered by a protective sheet which will reduce its absorption capabilities.

We propose to model MPPs as an equivalent fluid according to the Johnson-Champoux-Allard approach in combination with the FE method to simulate the sound absorbing behaviour of more complex MPP arrangements and to be able to predict MPP sound absorbing behavior in the frequency range beyond the cut-on frequency of a duct structure. The method relies on fitted model parameters of the MPP material under consideration. It shows that impedance tube data fitted material parameters acquired under normal incidence plane waves can be used to simulate more complex application scenarios if the geometry is fully resolved via the FE method.

Tests were carried out on various MPP configurations in an expansion chamber with variable attachment. The simulation of MPPs in these configurations show good agreement with measured TL-data.

## References


1. Maa, D.-Y., "Potential of Micro-Perforated Panel Absorber," *J. Acoust. Soc. Am.* 2861:104, 1998.
2. Morse, P.-M. and Ingard, K.-U., *Theoretical Acoustics*, (New York, McGraw-Hill, 1998), Chap. 9, 467pp., ISBN:978-0691024011.
3. Allard, J.-F. and Atalla, N., *Propagation of Sound in Porous Media: Modeling of Sound Absorbing Materials*, Second Edition, (Chichester, UK, Wiley, 2009), Chap. 3, 29pp., ISBN:978-0-47074-661-5.
4. Cox, T.-J. and D'Antonio, P., *Acoustic Absorbers and Diffusers: Theory, Design and Application*, Third Edition, (Florida, USA, CRC Press, Taylor & Francis, 2017), Chap. 6, 216pp., ISBN:978-1-4987-4099-9.
5. Atalla, N. and Sgard, F., "Modeling of Perforated Plates and Screens Using Rigid Frame Porous Media," *J. Sound Vib.* 303:195-208, 2007.
6. Allam, S. and Abom, M., "A New Type of Muffler Based on Microperforated Tubes," *J. Vib. Acoust.* 133:031005-1-031005-6, 2011.
7. Deutsches Institut für Normung, *DIN EN ISO 10534-2: Akustik - Bestimmung des Schallabsorptionsgrades und der Impedanz in Impedanzrohren; Teil 2: Verfahren mit Übertragungsfunktion* (Berlin: Beuth Verlag, 2010).
8. Jaouen, L. and Bécot, F.-X., "Acoustical Characterization of Perforated Facings," *J. Acoust. Soc. Am.* 129(3):1400-1406, 2011.
9. Randeberg, R.-T., "Perforated Panel Absorbers with Viscous Energy Dissipation Enhanced by Orifice Design," Ph.D. thesis, Department of Telecommunications, Norwegian University of Science and Technology, Trondheim, 2000.
10. Melling, T.-H., "The Acoustic Impedance of Perforates at Medium and High Sound Pressure Levels," *J. Sound. Vib.* 29(1):1-65, 1973.
11. Zwikker, C. and Kosten, C.-W., "*Sound Absorbing Materials*", (New York, Elsevier, 1999), Chap. 2, 25pp., ISBN:978-0-44440-661-3.
12. Allard, J.-F. and Champoux, Y., "New Empirical Equations for Sound Absorption Rigid Frame Porous Media," *J. Acoust. Soc. Am.* 91:3346, 1992.
13. Kaltenbacher, M., *Numerical Simulation of Mechatronic Sensors and Actuators*, Third Edition, (Heidelberg, Springer, 2015), Chap. 5, 159 pp, ISBN:978-3-642-40169-5.
14. Bolton, J.-S. and Hou, K., "Modeling of Perforated Plates and Screens Using Rigid Frame Porous Media," Purdue University, School of Mechanical Engineering, Publications of the R. W. Herrick Laboratories, 2009.
15. ASTM E2611-09, "Standard Test Method for Measurement of Normal Incident Sound Transmission of Acoustical Material Based on the Transfer Matrix Method," ASTM, 2006.
16. Kaltenbacher, M., "Fundamental Equations of Acoustics," In *Computational Acoustics*, First Edition, (Springer International Publishing, CISM International Centre for Mechanical Sciences, 2018). ISBN:978-3-319-59038-7.
17. Studiobox, "Schalldämmende Akustik-Studios," http://www.studiobox.de/professional-sprecherkabine-gesangskabine.html, accessed Nov. 2016.

## Contact Information

**Dipl.-Ing. Sebastian Floss**
Institute of Mechanics and Mechatronics/E325-A4
Vienna University of Technology
Getreidemarkt 9, 1060 Wien
Tel.: (+431) 58801 325415
sebastian.floss@tuwien.ac.at

## Abbreviations

**MPP** - Micro-perforated Panel

**HVAC** - Heating, Ventilation and Air-Conditioning

**FEM** - Finite Element Method

**TMM** - Transfer Matrix Method

**TL** - Transmission Loss

**SPL** - Sound Pressure Level



ISSN 0148-7191